Journal of Applied Sciences

ISSN 1812-5654

science alert

ANSInet
an open access publisher
http://ansinet.com

Journal of Applied Sciences 10 (13): 1255-1262, 2010
ISSN 1812-5654

Direct Partial Remelting of XW-42 Steel in Semi-Solid Zone

A. Alfan, M.Z. Omar, J. Syarif and Z. Sajuri
Department of Mechanical and Materials Engineering, Faculty of Engineering and Built Environment, Universiti Kebangsaan Malaysia 43600, Bangi, Selangor, Malaysia

Abstract: Microstructure that consists of spheroid grains in liquid matrix is desirable for semi-solid metal forming. In this study, a direct partial remelting from as annealed condition was used to examine microstructural evolution of XW-42 steel prior to thixoforming process. It was found out that M_7C_3 carbides dissolve inside the semi solid zone (between 1250-1270°C) while $M_{23}C_6$ carbides dissolve completely before entering semi-solid zone. The dissolution of these grain boundary carbides during partial remelting helps the grain spheroidisation of the XW-42 steel samples. Partial remelting at 1300 and 1340°C resulted in the formation of relatively spherical grains with liquid percent around 17%. The results indicate the suitability of these steel as a potential material for thixoforming through direct partial remelting route

Key words: XW-42 Steel, thixoforming, DTA, JMatPro, direct partial remelting

INTRODUCTION

Semi solid forming (also called thixoforming) is a new technology in which the metal is processed taking advantage of its thixotropic properties. In a thixotropic condition, an alloy can experienced a fall in viscosity if it is sheared but it will thicken again if it is allowed to stand. The first experiment to demonstrate this thixotropic behavior was conducted by Flemings and his co-workers in the early 1970s (Kirkwood, 1994). Since then, efforts have been made to put the new method at industrial level. The efforts were partially succeeded with utilization of thixoforming process to manufacture components made of low melting point alloys such as aluminium and magnesium alloys. One example of this component is space frame node for an Audi car structure made from MHD cast billets of AlMg5Si2Mn aluminium alloy (Hirt *et al*., 2009). Nevertheless, further development of Al and Mg alloys are still ongoing (Bayoumi *et al*., 2009; Chen *et al*., 2009).

On the other hand, development of high melting point material for thixoforming process hasn`t yet reached its goal (i.e., commercialization of steel thixoforming). However, efforts to realize the goal are steadily being pushed due to the benefits of steel thixoforming. Early studies mentioned that the benefits are low forging force compared to conventional forging process, possibility of forming components with complex and intricate shapes, reduction of steps in forming process, less air entrapment and also less shrinkage porosity compared to conventionally casting process (Omar *et al*., 2004a). Several steels have been investigated as potential thixoforming material candidates. The result seems promising for some steels such as X210CrW12 (Bramann *et al*., 2004; Seidl and Kopp, 2004; Uhlenhaut *et al*. 2006), AISI M2 tool steel (Omar *et al*., 2004b), 100Cr6 bearing steel (Bulte and Bleck., 2004; Seidl and Kopp, 2004) and high chromium cast iron (HCCI) (Huang *et al*., 2006). Other research on thixoforming of steels are focused on tools (Behrens *et al*., 2004; Kopp *et al*., 2004) and also supporting facilities for the process (Kuthe *et al*., 2004; Pierret *et al*., 2008).

Regarding these developments, however, research on thixoforming materials is still much needed to satisfy material selection process in order to bring steel thixoforming toward larger scale industrial application. XW-42 cold work tool steel is being studied in this research as a potential starting material for thixoforming process. The scope of this present study covers the microstructural evolution of XW-42 steel when the steel is directly heated to semi-solid zone from as annealed condition (Direct Partial Remelting)

EXPERIMENTAL PROCEDURE

Material: The material used in this work is an XW-42 cold work tool steel supplied in as-annealed condition (heated to 850°C, then cooled in the furnace at 10°C h^{-1} to 650°C, after that cooled freely in air). Chemical composition for

Corresponding Author: M.Z. Omar, Department of Mechanical and Materials Engineering, Faculty of Engineering and Built Environment, Universiti Kebangsaan Malaysia 43600, Bangi, Selangor, Malaysia Tel: +60389216031 0 Fax: +60389259659

the material was acquired using Foundry-Master Spark Spectrometer that is based on Optical Emission Spectroscopy (OES) method.

JMatPro simulation: JMatPro or Java-based Material Properties is software that was developed to augment the thermodynamic calculation by incorporating various theoretical material models and properties database that allow a quantitative calculation for the requisite materials property to be made within a larger software structure (Saunders *et al*., 2003). A modified Scheil-Guliver model is employed by the software to perform the simulation. By using this model, liquid fraction profile as well as phase stability diagram can be created.

DTA measurement: DTA measurement was carried out to estimate solidus and liquidus temperatures as well as liquid fraction profile within the semi-solid zone and carbide stability zone of studied material. The measurement was performed using Netzsch Simultaneous Thermal Analysis (STA) 409°C equipment. The sample was cut into small pieces with total weight of 50-100 mg with alumina as reference material. Heating rate of 5°C min^{-1} was employed for the test. The solidus and liquidus temperatures as well as liquid fraction profile were constructed using Proteus software (Puttgen and Bleck, 2004).

Direct partial remelting experiment: The direct partial remelting experiment was performed using vertical, high temperature carbolite furnace. The material was cut into coupons of 5×10×12 mm. For each test, a coupon was hung inside the furnace by using chromel wire. To ensure that coupon was heated into designated temperature, a K-type thermocouple was placed nearby the coupon without making any direct contact with the coupons to prevent damages to the thermocouple. The tests were repeated for various selected temperatures (based on liquid fraction profiles from DTA measurement) with fixed holding time of 2 min and subsequently quench into brine solution to freeze the structures. The heating was carried out in an argon atmosphere to reduce oxidation. Heating rate of the furnace was found to be around 20°C min^{-1}.

Metallography and image analysis: Coupons from direct partial remelting experiments were ground and polished to get clean and mirror-like surface. Subsequently, the coupons were etched using Villela reagent (1 g picric acid, 5 mL hydrochloric acid and 95 mL ethyl alcohol) to reveal their microstructures. Microstructures observation and analysis were conducted by using BX-51 Olympus optical microscope as well as Hitachi S3400N scanning electron microscope (SEM), equipped with Energy Dispersive Spectroscopy (EDX) to analyze chemical composition of the selected area/spots. EDX identifies chemical composition of the selected area/spots by recognizing x-ray in which its energy amount is unique for every element (Goldstein *et al*., 1981).

RESULTS AND DISCUSSION

Starting material: Table 1 shows chemical analysis result for XW-42 steel. Standard specification (Steiner and American Society for Metals, 1990) confirmed that chemical analysis result from the alloy fall within the required standard. Optical micrographs of as received sample are shown in Fig. 1a and b. It shows arrays of large carbides with smaller carbides distributed homogeneously. This structure is known to be found in an annealed cold work tool steel (Roberts *et al*., 1971) thus confirms that soft annealing treatment has been done as described by the material supplier. According to Roberts *et al*. (1971), the carbides in XW-42 steel (designated as D2 by AISI) are mostly from M_7C_3 type carbide which is confirmed by JMatPro simulation (Fig. 2). Beside the predominant M_7C_3 type carbide, JMatPro simulation also estimates the existence of MC and $M_{23}C_6$ types of carbide in this steel. However the amount of both types of carbides after cooling to room temperature is negligible compare to M_7C_3 carbides.

SEM observation using back scattered mode was used to analyze the carbides of the starting material in detail (Fig. 1c). It was found that both large carbides and small carbides are darkish in appearances, indicating their similarity in major constituent elements. EDX analysis has been performed to analyze the type of carbides based on their chemical composition (Table 2). It is found that the darkish carbides are rich in chromium and iron with atomic proportion between carbon and other metallic elements (Fe, Cr, Mo and V) reaches 3:7 ratio. Hence the darkish carbides analyzed thus far (Table 2) are most likely an M_7C_3-type carbide. M_7C_3 and $M_{23}C_6$ carbides cannot being distinguished based on back scattered imaging mode because both are Cr-rich type carbides (Laigo *et al*., 2008).

Table 1: Chemical composition of XW-42 Steel (wt. %)

	C	Si	Mn	Cr	Ni	Mo	V
Test result	1.46	0.258	0.239	11.2	0.197	0.769	0.711
Standard (Steiner and American Society for Metals, 1990)	1.4-1.6	0.600 (Max.)	0.600 (Max.)	11-13	0.300 (Max.)	0.7-1.2	1.100

Table 2: EDX analysis results of the darkish carbides

	Chemical composition (at%)				
Spot at Fig. 1c	C	V	Cr	Fe	Mo
1	31.76	2.77	33.21	31.75	0.52
2	31.13	1.69	33.99	32.61	0.58
3	32.54	1.84	32.76	32.34	0.53

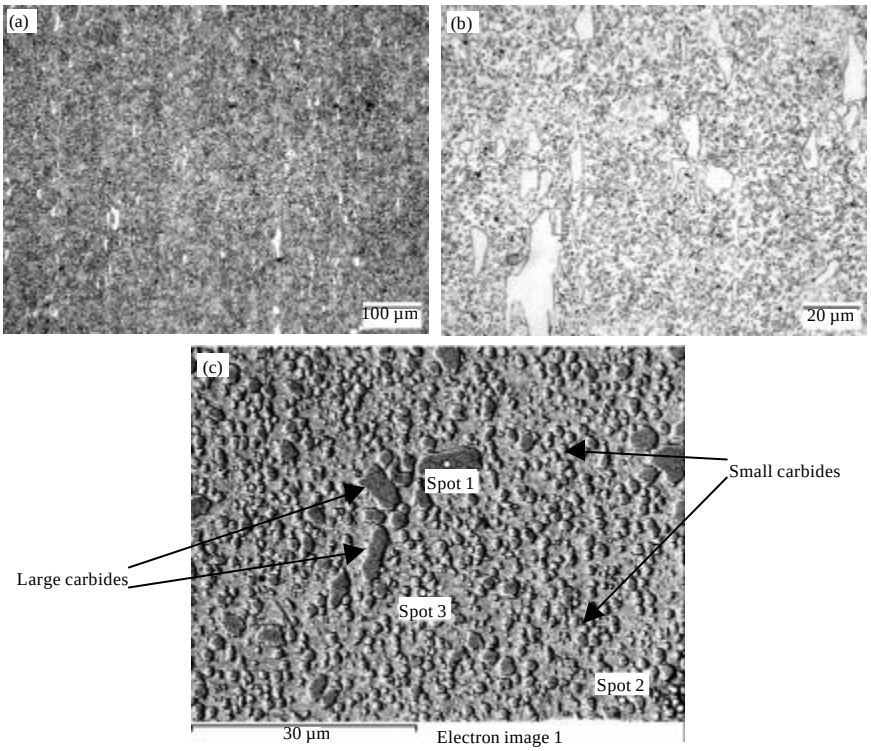

Fig. 1: Micrographs of As-Received XW-42 Steel from (a, b) Optical Microscope and (c) SEM

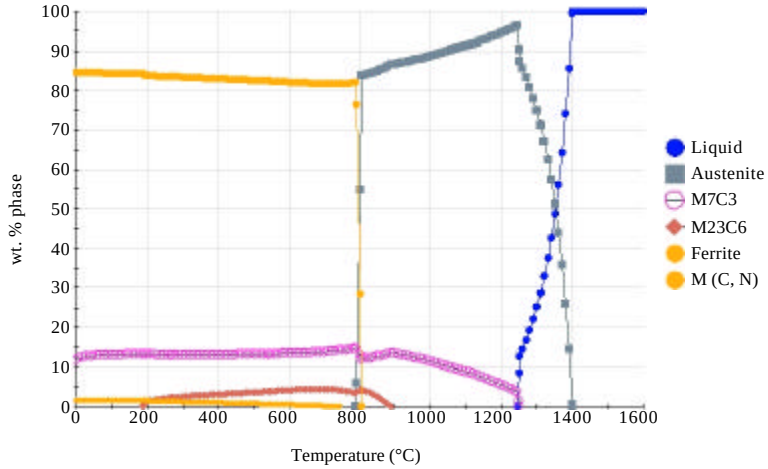

Fig. 2: Phase equilibrium diagram of XW-42 steel obtained from JMatPro simulation

Note that phases that are rich in elements with high atomic numbers such as W and Ta (to name a few) will appear bright in Fe matrix, while those that are rich in elements with low atomic numbers, such as Cr and V, will appear greyish or darkish (Goldstein *et al*., 1981). Furthermore, as will be later explained, the carbide of importance in this study will be the M_7C_3-type carbide, as it has given a huge influenced to the grain boundary liquation when heated into the semi-solid zones.

Estimation of semi-solid temperature interval: Liquid Fraction Profile (LFP) of XW-42 steel from DTA measurement and also from JMatPro simulation is shown in Fig. 3. The solidus line for this alloy is estimated at

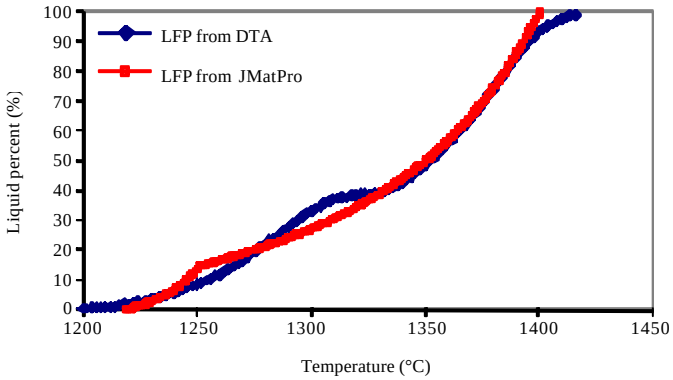

Fig. 3: Liquid fraction profile of XW-42 steel obtained from DTA and JMatPro simulation

1200-1220°C while the liquidus temperature is at 1400°C. Plateau shape is found on both curves but at different temperature and liquid fraction ranges. For LFP created from DTA measurement, the plateau shape is found at 1300-1343°C that corresponds to liquid percent around 40%. Whereas for LFP from JMatPro, the plateau shape is found rather earlier at 1250-1260°C that corresponds to liquid percent around 15%. The plateau shape becomes an advantage in semi solid metal forming due to its low fluctuation in liquid fraction at given temperature range, thus makes the forming process easier. Previous work discovered that such plateau shape is caused by dissolution of certain carbide(s) inside semi-solid zone (Puttgen and Bleck, 2004; Omar *et al*., 2009; Meuser and Bleck, 2001). By using the phase equilibrium diagram in Fig. 2 and also explanation about types of carbides in as received sample above, it is strongly believed that the carbides that dissolved at this plateau region are M_7C_3 carbides.

Temperatures for partial re-melting experiment were selected based on the liquid fraction profile. The experiment were performed at sub solidus (1190°C) and at semi-solid zone (1220, 1250, 1270, 1300 and 1340°C) The selected temperatures are up to 50% liquid percent that was said to be the upper limit of liquid percent for thixoforming process (Omar *et al*., 2004a). Above this limit, some alloys exhibits fall in viscosity value which could be detrimental to its thixotropic behaviour (Kirkwood, 1994).

Microstructures in sub-solidus and semi-solid zone: Microstructures of XW-42 Steel at 1190°C and 1220°C are shown in Fig. 4 a-c. By comparing Fig. 1c and 4c, it could be seen that at 1190°C some of the darkish carbides have already dissolved. It was believed that the dissolved carbides are all $M_{23}C_6$ carbides along with some M_7C_3 carbides. Thus, the remaining darkish carbide could be positively confirmed as M_7C_3 carbides due to its high dissolution temperature. EDX examination results also support the claim by obtaining the similar carbide chemical composition as in Table 2. Other than carbides, equiaxed austenite grains are also observed, especially at the SEM micrograph (Fig. 4c). However, it is only partly visible due to etchant attacking preference effect.

At 1250°C (Fig. 5 a) the M_7C_3 carbides start to dissolve more rapidly and the equiaxed austenite grains in background are now more visible. Also at this temperature, liquid phase should be appearing at around 10% volume fraction according to DTA profile at Fig. 3. However, due its low quantity of liquid phase (<25% volume fraction), partial remelting experiment failed to reveal the presence of liquid phase other than thin film of dark phase at the grain boundaries (Fig. 5a). This is attributed to insufficient cooling rates during quenching that enables the liquid phase at the vicinity of grains to solidify epitaxially (Tzimas and Zavaliangos, 2000a).

An increase in partial remelting temperature to 1270°C will dissolve all remaining M_7C_3 carbides. Furthermore, dark eutectics formed from quenched liquid phase start to appear at this temperature, indicating the much reduced epitaxial effect due to significant increase in liquid phase (up to 17% according to Fig. 3). Calculation on the dark eutectics phase (LFP from image analysis) observed at Fig. 7 shows that its average volume fraction reaches 12%. However, the dark eutectics seem to be grouped along rolling direction and not dispersed around the grains.

Further heating to 1300 and 1340°C (Fig. 6a, b) increases the dark eutectics volume fractions to around 17% due to increase in liquid phase up to 40% according LFP in Fig. 3. The increase of dark eutectics volume fraction, which represents the increase of liquid phase, is thought to give a significant surface tension that affect grain size and spheroidity level. The grain spheroidity

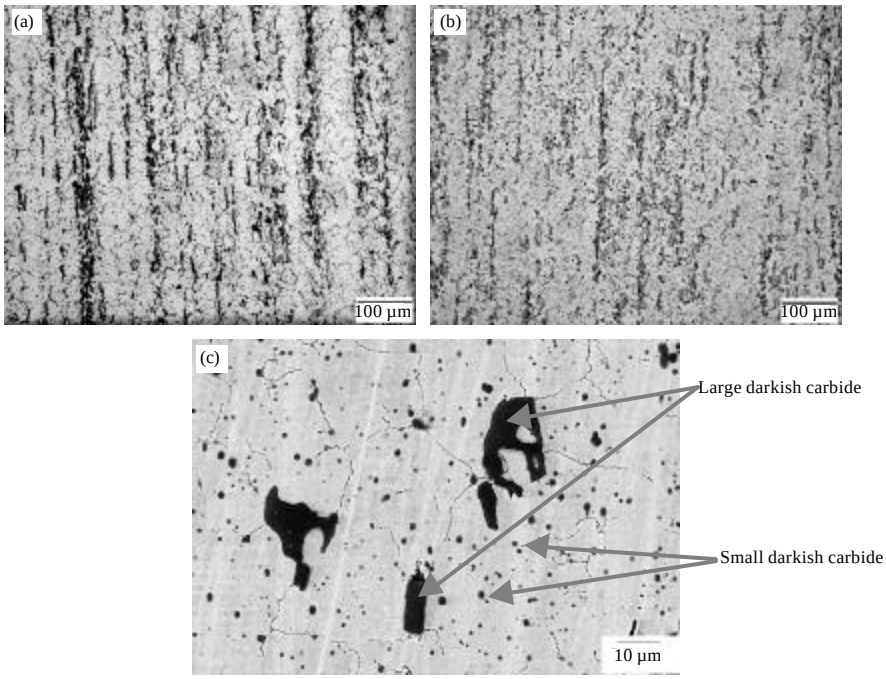

Fig. 4: Micrographs of XW-42 steel at (a) 1190°C and (b) 1220°C while (c) is the SEM micrograph at 1190°C showing M7C3 carbides

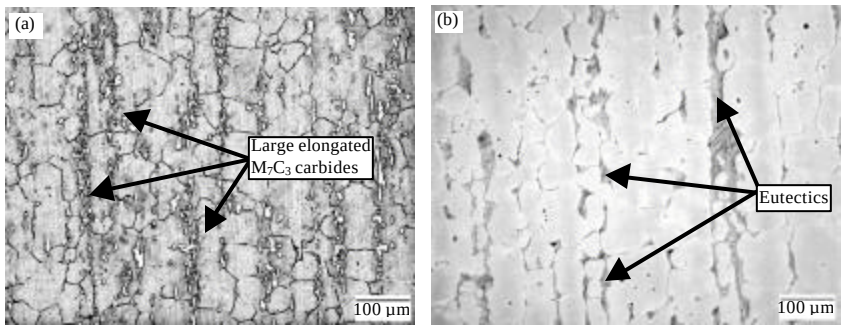

Fig. 5: Optical micrographs of XW-42 steel at (a) 1250°C and (b) 1270°C

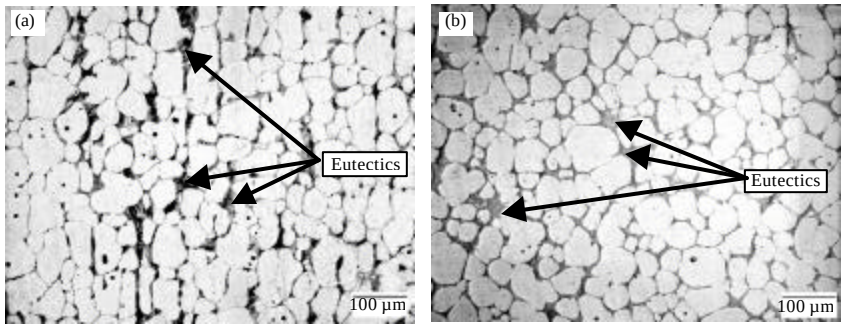

Fig. 6: Optical micrographs of XW-42 steel at (a) 1300°C and (b) 1340°C

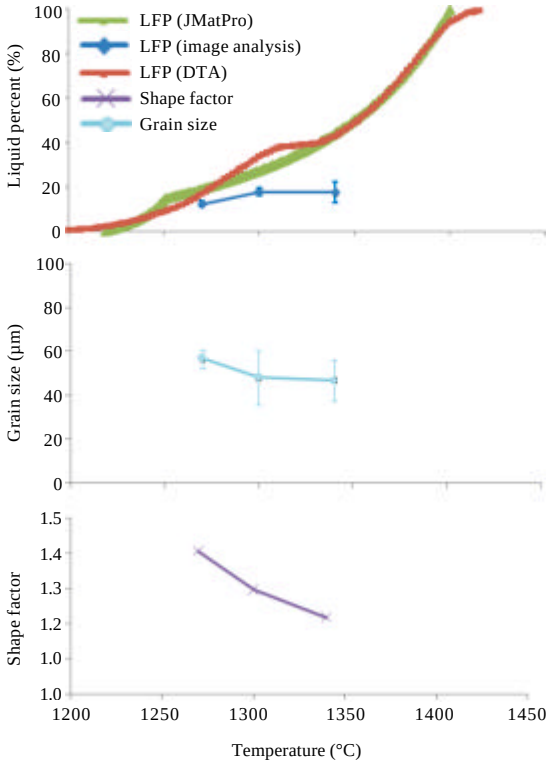

Fig. 7: Relation between liquid fraction profile, average grain diameter and shape factor of XW-42 steel at semi-solid zone

level is calculated by using shape factor equation (Bergsma *et al*., 1997):

$$F = \frac{U^2}{4\pi A} \quad (1)$$

where, F is the shape factor, U is the grain circumference and A is the grain area. In the case of F =1, the grains are fully spherical, while for more complex shape, the shape factor is >1.

Figure 7 shows the effect of partial remelting temperature at 1270, 1300 and 1340°C to the average grain sizes and shape factor of the austenite grains. The average grain diameters at these temperatures are found to be around 40-60 μm. It is found that increase in partial remelting temperature will reduce the grain size due to melting at the sharp asperities of the equiaxed grains that is preceded by liquid penetration into the grain boundaries. Then the melting is followed by solidification in regions of negative curvature due to diffusion (Omar *et al*., 2009). Hence, the reduction of the grain size is resulted in the decline of shape factor value, which

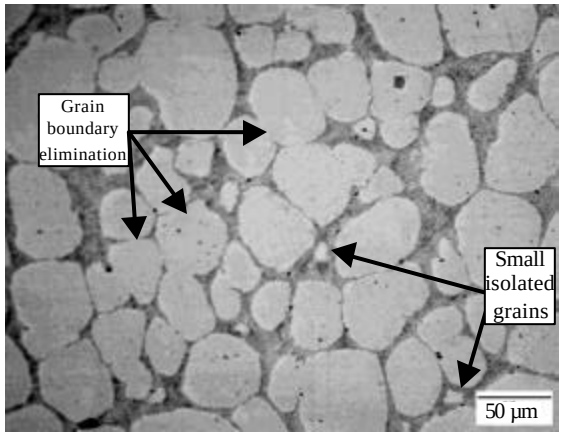

Fig. 8: Grain agglomeration at 1340°C that leads to grain boundary elimination. Small unattached isolated grains will be slowly liquidated due to Otswald Ripening

means better grain spheroidity level. However, it also can be proven that for other alloys (such as AISI M2), grain growth can overcome the reduction process and will result in bigger grain at higher partial remelting temperatures without sacrificing its spheroidity (Omar *et al*., 2009).

Grain agglomeration occurs for some grains at semi-solid zone as depicted at Fig. 8. Agglomerates could have a beneficial effect for thixoforming process by creating solid skeleton structure that will support the alloy in high liquid content condition (Tzimas and Zavaliangos, 2000b). Previous works show that the agglomerate consists of grains connected with low angle grain boundary (i.e., with misorientation less than 10°) (Liu *et al*., 2005; Arnberg *et al*., 1999). Subsequent process of grain rotation and/or grain boundary migration minimizes the misorientation and then eliminates the grain boundary line. On the other hand, isolated unattached grains will be liquidated and become smaller due to Otswald ripening process (Tzimas and Zavaliangos, 2000b).

In order to examine the suitability of an alloy for thixoforming based on its microstructure prior to forming process, specific criterions for average grain size and shape factor is used. Uggowitzer *et al*. (2000) specified that the average grain size of an alloy must not exceed 100 μm, while its shape factor must be below 2 in order to have good mould filling behavior (Bünck *et al*., 2009). By using this criterions, it is apparent that the average grain sizes and shape factor for XW-42 steel at 1270, 1300 and 1340°C are suitable for thixoforming process because they are in the range of 50-60 μm and 1.2-1.4, respectively

(which is well below the limit value of grain size and shape factor at 100 μm and 2, respectively). However, unbalanced liquid phase distribution found at 1270°C is thought to be detrimental for thixoforming process owing to its lack of wetting effect during forming process. Hence, higher temperature (such as at 1300 and 1340°C) is more recommended for forming process.

CONCLUSION

The microstructural evolution of XW-42 steel has been examined using direct partial remelting experiment. The as-received material shows arrays of large carbides with smaller carbides distributed homogeneously. The carbides were identified as M_7C_3 and $M_{23}C_6$ carbides. Further heating to sub solidus zone at 1190°C reveals the dissolution of $M_{23}C_6$ carbides while the M_7C_3 carbides are still observed after entering semi solid zone and finally dissolve between 1250-1270°C. Epitaxial effect during quenching reduces significantly the volume fraction of dark eutectics that represents the liquid phase. Subsequent calculation after partial remelting shows that the liquid fraction at 1250°C is 12% and increase to 17% at 1300-1340°C. Equiaxed grains found at 1250°C have transformed into more spherical grains at higher partial remelting temperatures (i.e., 1270, 1300 and finally 1340°C). Based on criterions for average grain size and shape factor and also acknowledging the distribution of the liquid phase around grains, it could be said that structures at 1300 and 1340°C are thought to be suitable for thixoforming process.

ACKNOWLEDGMENT

The authors would like to thank to Universiti Kebangsaan Malaysia (a.k.a. National University of Malaysia) and Ministry of Science, Technology and Innovation (MOSTI) Malaysia for sponsoring this work.

REFERENCES

Arnberg, L., A. Bardal and H. Sund, 1999. Agglomeration in two semisolid type 6082 aluminium alloys. Mater. Sci. Eng., A262: 300-303.

Bayoumi, M.A., M.I. Negm and A.M. El-Gohry, 2009. Microstructure and mechanical properties of extruded Al-Si alloy (A356) in the semi-solid state. Mater. Des., 30: 4469-4477.

Behrens, B., B. Haller and D. Fischer, 2004. Thixoforging of steel using ceramic tool materials. Steel Res. Int., 75: 561-568.

Bergsma, S.C., M.C. Tolle, M.E. Kassner, X. Li and E. Evangelista, 1997. Semi-solid thermal transformations of Al-Si alloys and the resulting mechanical properties. Mater. Sci. Eng., 237: 24-34.

Bramann, H., C. Afrath, T. Grimmig, M. Fehlbier and A. Bührig-Polaczek, 2004. Casting of high alloy steels in the mushy state. Steel Res. Int., 75: 537-544.

Bulte, R. and W. Bleck, 2004. Effects of pre-processing on thixoformability of steel grade 100Cr6. Steel Res. Int., 75: 588-592.

Bünck, M., F. Küthe and A. Bührig-Polaczek, 2009. Rheocasting of Aluminium and Thixocasting of Steel. In: Thixoforming-Semi-Solid Metal Processing, Hirt, G. and R. Kopp (Eds.). Willey-VCH Verlag GmbH, USA., pp: 311-368.

Chen, T.J., Y. Ma, B. Li, Y.D. Li and Y. Hao, 2009. Effects of processing parameters on wear behaviors of thixoformed AZ91D magnesium alloys. Mater. Des., 30: 235-244.

Goldstein, J.I., D.E. Newbury, P. Echlin, D.C. Joy, C. Fiori and E. Lifshin, 1981. Scanning Electron Microscopy and X-Ray Microanalysis, A Text for Biologists, Materials Scientists and Geologists. 1st Edn., Plenum Press, New York.

Hirt, G., L. Khizhnyakova, R. Baadjou, F. Knauf and R. Kopp, 2009. Semi-Solid Forming of Aluminium and Steel-Introduction and Overview. In: Thixoforming-Semi-Solid Metal Processing, Hirt, G. and R. Kopp (Eds.). Willey-VCH Verlag GmbH, USA., pp: 1-27.

Huang, Z., J. Xing and A. Zhang, 2006. Investigation of microstructure and impact toughness of semisolid hypereutectic high chromium cast iron prepared by slope cooling body method. J. Applied Sci., 6: 1635-1640.

Kirkwood, D.H., 1994. Semisolid metal processing. Int. Mater. Rev., 39: 173-189.

Kopp, R., H. Shimahara, J.M. Schneider, D. Kurapov, R. Telle and S. Münstermann, 2004. Characterization of steel thixoforming tool materials by high temperature compression tests. Steel Res. Int., 75: 569-576.

Kuthe, F., A. Schonbohm, D. Abel and R. Kopp, 2004. An automated thixo-forging plant for steel parts. Steel Res. Int., 75: 593-600.

Laigo, J., F. Christien, R. Le Gal, F. Tancret and J. Furtado, 2008. SEM, EDS, EPMA-WDS and EBSD characterization of carbides in HP type heat resistant alloys. Mater. Characterization, 59: 1580-1586.

Liu, D., H.V. Atkinson and R.L. Higginson, 2005. Disagglomeration in thixoformed wrought aluminium alloy 2014. Mater. Sci. Eng., 392: 73-80.

Meuser, H and W. Bleck, 2001. Microstructural investigations in the semi-solid state of the steel X210CrW12. Steel Res. Int., 72: 271-276.

Omar, M.Z., H.V. Atkinson, E.J. Palmiere, A.A. Howe and P. Kapranos, 2004a. Microstructural development of HP9/4/30 steel during partial remelting. Steel Res. Int., 75: 552-560.

Omar, M.Z., E.J. Palmiere, A.A. Howe, H.V. Atkinson and P. Kapranos, 2004b. Thixoforming of GFM M2 tool steel from the as-annealed condition. Proceeding of the 8th International Conference on Semi-Solid Processings of Alloys and Composites, (ICSSPAC'04), Limassol, Cyprus, pp: 521-531.

Omar, M.Z., H.V. Atkinson, A.A. Howe, E.J. Palmiere, P. Kapranos and M.J. Ghazali, 2009. Solid-liquid structural break-up in M2 tool steel for semi-solid metal processing. J. Mater. Sci., 44: 869-874.

Pierret, J.C., A. Rassili, G. Vaneetveld, J. Lecomte-Beckers and R. Bigot, 2008. Robustness of a thixoforming production line. Solid State Phenomena, 141-143: 207-212.

Puttgen, W. and W. Bleck, 2004. DTA-Measurements to determine the thixoformability of steels. Steel Res. Int., 75: 531-536.

Roberts, G.A., J.C. Hamaker and A.R. Johnson, 1971. Tool Steels. 2nd Edn., ASM, USA.

Saunders, N., Z. Guo, X. Li, A.P. Miodownik and J. Schillé, 2003. Using *JmatPro* to model materials properties and behavior. JOM J. Minerals Metals Mater. Soc., 12: 60-65.

Seidl, I. and R. Kopp, 2004. Semi-solid rheoforging of steel. Steel Res. Int., 75: 545-551.

Steiner, R. and American Society for Metals, 1990. ASM Handbook Volume 1: Properties and Selection: Irons, Steels and High-Performance Alloys. 10th Edn., ASM International, USA., ISBN-10: 0871703777.

Tzimas, E. and A. Zavaliangos, 2000a. Evaluation of volume fraction of solid in alloys formed by semi-solid processing. J. Mater. Sci., 35: 5319-5330.

Tzimas, E. and A. Zavaliangos, 2000b. Evolution of near-equiaxed microstructure in the semi-solid state. Mater. Sci. Eng., 289: 228-240.

Uggowitzer, P.J., G. Gullo and A. Wahlen, 2000. Metallkundliche aspekte der semi-solid formgebung von leichtmetallen. First Ranshofener Leichtmetalltage. http://e-collection.ethbib.ethz.ch/eserv.php?pid=eth:25645&dsID=eth-25645-01.pdf.

Uhlenhaut, D.I., J. Kradolfer, W. Püttgen, J.F. Löffler and P.J. Uggowitzer, 2006. Structure and properties of a hypoeutectic chromium steel processed in the semi-solid state. Acta Materialia, 54: 2727-2734.